

The Effect of Pressure on Diffusion in Water and in Sulfate Solutions

R. B. CUDDEBACK, R. C. KOELLER, AND H. G. DRICKAMER*

Department of Chemistry, University of Illinois, Urbana, Illinois

(Received September 26, 1952)

Diffusion coefficients are presented as a function of pressure to 10 000 atmospheres for the following systems:

THO—H ₂ O	0°–25°–50°;
0.1 N H ₂ S ³⁵ O ₄ —0.1 N H ₂ SO ₄	0°–5°–25°–50°;
0.1 N Na ₂ S ³⁵ O ₄ —0.1 N Na ₂ SO ₄	0°–25°–50°;
1.0 N Na ₂ S ³⁵ O ₄ —1.0 N Na ₂ SO ₄	0°–25°–50°;
0.1 N K ₂ S ³⁵ O ₄ —0.1 N K ₂ SO ₄	0°–25°–50°.

The results are interpreted in terms of the activation volume and the tetrahedrally coordinated structure of water. It is found that pressure tends to break down the structure, and in certain regions an increase in diffusion coefficient with pressure is noted.

In the salt solutions the water structure is controlling with some added effects due to solvation and ionic interaction.

IN previous papers^{1,2} a method for measuring diffusion in liquids under pressures to 10 000 atmospheres was presented, along with results for some organic solutions. In this paper results are presented for diffusion of tritiated water into ordinary water, for diffusion of S³⁵ tagged 0.1 N sulfuric acid into untagged 0.1 N sulfuric acid, and for diffusion in 0.1 N Na₂SO₄, 1.0 N Na₂SO₄, and 0.1 N K₂SO₄. The tritiated water was obtained from Tracerlab, the S³⁵ tagged H₂SO₄ from Oak Ridge National Laboratory of the U. S. Atomic Energy Commission. The ordinary water was de-ionized, and degassed water was obtained from the Boiler Water Laboratory by courtesy of F. G. Straub. The salts were cp quality.

The method of operation and for calculation of the diffusion coefficients is completely discussed in reference 1. The kinetic theory of liquids and the method for calculating the enthalpy of activation (ΔH^\ddagger), the entropy of activation (ΔS^\ddagger) above the value at atmospheric pressure (ΔS_0^\ddagger), the activation volume (ΔV^\ddagger), and the free energy of activation (ΔF^\ddagger) are discussed in references 1 and 2.

The results will be discussed in terms of these concepts. The data are shown in Tables I–V.

SELF-DIFFUSION IN WATER

In Fig. 1 the diffusion coefficients are plotted against density using Bridgman's³ compressibility data. The excellent agreement with the data of Orr and Butler⁴ at atmospheric pressure is to be noted. As a matter of fact, the fritted glass was calibrated using their data at 25°C. Since each isotherm has a unique shape, it is ap-

* This work was supported in part by the U. S. Atomic Energy Commission.

¹ R. C. Koeller and H. G. Drickamer, J. Chem. Phys. 21, 267 (1953).

² R. C. Koeller and H. G. Drickamer, J. Chem. Phys. 21, 575 (1953).

³ P. W. Bridgman, *The Physics of High Pressure* (Macmillan Company, New York, 1931).

⁴ W. J. C. Orr and J. A. V. Butler, J. Chem. Soc. (London) 1935, 1273.

parent that the molecular geometry and mechanisms of motion depend upon more than merely density. This system will be analyzed primarily on the basis of changes in the activation volume. The activation volume is purely a function of a single isotherm, whereas ΔH^\ddagger and ΔS^\ddagger depend upon the displacements between the three isotherms. The structure obviously varies radically with temperature and thus ΔH^\ddagger and ΔS^\ddagger calculated on the basis of the three isotherms probably do not apply to any of them.

TABLE I. Measured diffusion coefficients for THO in H₂O.^a

Temp. °K	Pressure atmos	Effective cell length cm	Observed $D \times 10^5$ cm ² /sec
273	136	0.504	1.65
273	252	0.504	2.37
273	600	0.504	1.06
273	900	0.504	1.84
273	1240	0.504	1.45
273	2040	0.557	1.08
273	3500	0.557	0.787
273	5900	0.611	0.584
298	1	0.504	2.64
298	245	0.504	2.90
298	1300	0.504	3.24
298	2050	0.557	3.06
298	2500	0.557	3.04
298	3000	0.557	2.62
298	3000	0.557	2.36
298	3975	0.557	1.71
298	5000	0.557	1.15
298	7000	0.611	0.753
298	7000	0.611	0.843
298	9175	0.611	0.515
323	235	0.504	5.15
323	735	0.504	4.17
323	1300	0.504	3.48
323	2100	0.557	2.33
323	2500	0.557	1.86
323	2500	0.557	1.89
323	3500	0.557	1.82
323	4450	0.557	2.07
323	7000	0.611	2.25
323	10050	0.665	1.38

^a Maximum deviation in reproducibility 10 percent. Average deviation 5 percent.

TABLE II. Measured diffusion coefficients for $0.1 N H_2S^{34}O_4$ in $0.1 N H_2SO_4$.^a

Temp. °K	Pressure atmos	Effective cell length cm	Observed $D \times 10^5$ cm ² /sec
273	238	0.504	0.678
273	338	0.504	0.265
273	500	0.504	0.506
273	666	0.504	0.836
273	800	0.504	0.956
273	1340	0.504	0.764
273	1850	0.557	0.786
273	2500	0.557	0.656
273	4050	0.557	0.650
273	5500	0.611	0.415
278	100	0.504	1.05
278	250	0.504	0.940
278	303	0.504	0.741
278	355	0.504	0.956
278	515	0.504	1.38
278	1000	0.504	0.982
298	238	0.504	2.22
298	370	0.504	2.36
298	803	0.504	2.62
298	1000	0.504	2.47
298	3000	0.557	1.76
298	5000	0.557	1.13
298	6850	0.611	0.721
298	8500	0.611	0.502
323	524	0.504	3.20
323	1500	0.504	3.11
323	2050	0.611	2.67
323	3400	0.557	2.47
323	5100	0.611	1.66
323	6900	0.611	1.13
323	8900	0.665	0.806
323	10150	0.665	0.631

^a Maximum deviation in reproducibility 10 percent. Average deviation 5 percent.

TABLE III. Diffusion coefficients, $0.1 N Na_2S^{35}O_4 - 0.1 N Na_2SO_4$.^a

Temp. °K	Pressure atmos	Effective cell length cm	Observed $D \times 10^5$ cm ² /sec
273	100	0.548	0.99
273	238	0.548	0.91
273	377	0.548	0.59
273	510	0.548	1.08
273	652	0.548	0.84
273	803	0.548	0.69
273	1304	0.548	0.72
273	1650	0.617	0.65
273	2050	0.617	0.54
273	4000	0.617	0.49
273	6000	0.676	0.47
298	1	0.676	1.41
298	252	0.548	1.58
298	640	0.548	1.92
298	1200	0.548	2.18
298	1900	0.617	2.89
298	2500	0.617	1.92
298	4550	0.617	1.16
298	6525	0.676	1.27
298	9000	0.676	0.96
323	120	0.548	4.32
323	510	0.548	2.90
323	1005	0.548	2.25
323	1950	0.617	1.44
323	2500	0.617	1.43
323	3500	0.617	2.93
323	4500	0.617	1.75
323	7000	0.724	1.52
323	10500	0.724	1.30

^a Maximum deviation in reproducibility 15 percent. Average deviation 5 percent.

TABLE IV. Diffusion coefficients, $1 N Na_2S^{36}O_4 - 1 N Na_2SO_4$.^a

Temp. °K	Pressure atmos	Effective cell length cm	Observed $D \times 10^5$ cm ² /sec
273	20	0.548	0.28
273	210	0.548	0.33
273	400	0.548	0.29
273	600	0.548	0.39
273	1000	0.548	0.56
273	1800	0.548	0.91
273	3050	0.617	0.55
298	34	0.548	0.90
298	238	0.548	1.01
298	238	0.548	0.86
298	605	0.548	0.76
298	1000	0.548	1.07
298	2000	0.617	1.60
298	3225	0.617	0.78
298	4500	0.617	1.03
298	6050	0.676	0.80
323	20	0.548	4.86
323	265	0.548	1.24
323	640	0.548	1.14
323	1000	0.548	1.34
323	2200	0.617	1.88
323	3000	0.617	2.24
323	3000	0.617	2.27
323	4050	0.617	1.46
323	5100	0.617	1.26
323	6550	0.724	1.81
323	6950	0.676	1.54
323	10000	0.724	1.25

^a Maximum deviation in reproducibility 15 percent. Average deviation 5 percent.

TABLE V. Diffusion coefficients, $0.1 N K_2S^{35}O_4 - 0.1 N K_2SO_4$.^a

Temp. °K	Pressure atmos	Effective cell length cm	Observed $D \times 10^5$ cm ² /sec
273	10	0.548	0.33
273	100	0.548	0.67
273	265	0.548	0.71
273	390	0.548	0.50
273	415	0.548	0.40
273	600	0.548	0.90
273	775	0.548	0.86
273	1060	0.548	0.83
273	1800	0.548	0.82
273	3075	0.617	0.66
298	100	0.548	1.40
298	252	0.548	0.98
298	258	0.548	1.04
298	610	0.548	1.30
298	610	0.548	1.44
298	1000	0.548	0.90
298	1210	0.548	0.84
298	1900	0.548	1.17
298	2850	0.617	1.59
298	3800	0.617	0.82
298	4650	0.617	0.87
323	100	0.548	3.92
323	230	0.548	2.48
323	1000	0.548	0.87
323	1500	0.548	0.75
323	1970	0.548	1.46
323	3000	0.617	2.06
323	4050	0.617	2.37
323	4950	0.617	1.44
323	6550	0.676	1.04
323	10250	0.724	0.58

^a Maximum deviation in reproducibility 10 percent. Average deviation 5 percent.

From studies, the tetrahedral that decreases tend in the sol valence fo regular st consists over cules with changing. extra hyd between ordinary i The rat volume is Fig. 2. The 25° is with the i



FIG. 1. I

This indic is broken of the mo and 1 atr conclude that whe collapse. molecules ture app proaching approach atmos), sion decre is now c the incre than the ture. In because felt thro is decre to decre

From spectroscopic, dielectric, and x-ray diffraction studies, the modern view of water is that it retains the tetrahedrally coordinated structure of ice to a degree that decreases with increasing temperature. The molecules tend to arrange themselves in a tetrahedral manner in the solid because of the particular distribution of valence forces about the molecule. Upon melting, the regular structure is not completely destroyed, but persists over regions including tens or hundreds of molecules with the membership of the groups continually changing. The oxygen atoms tend to coordinate an extra hydrogen so that "hydrogen bonds" are formed between molecules. These bonds are stronger than ordinary intermolecular attractive forces.

The ratio of the activation volume to the molal volume is plotted for the three isotherms studied in Fig. 2. The compressibility data of Bridgman³ was used. The 25° isotherm of $\ln D$ in Fig. 1 shows the D increases with the initial increase of pressure above atmospheric.

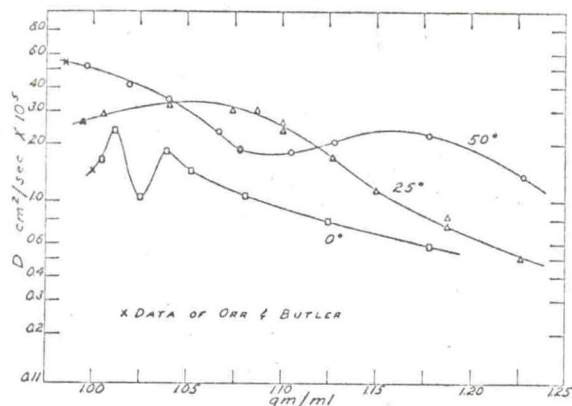


FIG. 1. Diffusion coefficients for the system THO-H₂O as a function of density.

This indicates that the tetrahedral structure in the water is broken down by pressure so that the average mobility of the molecules increases. The activation volume of 25° and 1 atmos is seen to be negative. From this we can conclude that the tetrahedral structure must be such that when a molecule migrates there is a localized collapse. As pressure is increased the percentage of molecules held in the characteristic tetrahedral structure apparently decreases and we find D slowly approaching a maximum while the activation volume approaches zero. Then, at the maximum in D (1500 atmos), $\Delta V^\ddagger/\bar{V}$ passes through zero. Further compression decreases D either because the tetrahedral structure is now completely destroyed, or because the effect of the increased compactness of the medium is greater than the influence of whatever remains of the structure. In any event, the activation volume increases because the local expansion necessary for activation is felt through a greater portion of the fluid as free volume is decreased. At 4000 atmos the slope of $\ln D$ vs P begins to decrease rather than increase and $\Delta V^\ddagger/\bar{V}$ goes

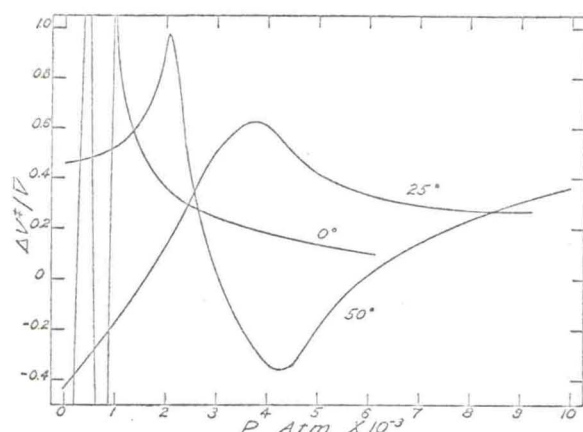


FIG. 2. Activation volume as a function of pressure. System: THO-H₂O.

through a maximum of 63 percent. The occurrence of this maximum and the relatively slow decrease of $\ln D$ and $\Delta V^\ddagger/\bar{V}$ beyond it indicate that a stabilized structure is forming in the same sense that such structures were formed in the organic solutions.^{1,2} That is, the configuration is becoming increasingly difficult to deform (either with increased pressure or during activation for diffusion), and diffusion takes place more and more through existing holes. Thus, we see that the activation volume settles down to approach an asymptote of about 25 percent of the molal volume.

Activation enthalpies are plotted versus pressure for 285, 298, and 310°K in Fig. 3. The change in activation entropy with pressure was calculated and is shown graphically in Fig. 4. The changes in ΔH^\ddagger and ΔS^\ddagger calculated for the 25° isotherm are probably reasonably correct since 25° is the median temperature. With the initial application of pressure the structure begins to be broken down to decrease the order and increase the entropy level of the normal state. Thus, we see that the activation entropy (the difference between entropy levels of the initial and activated states) decreases in this range to a minimum of 17 cal/°K/mole below that

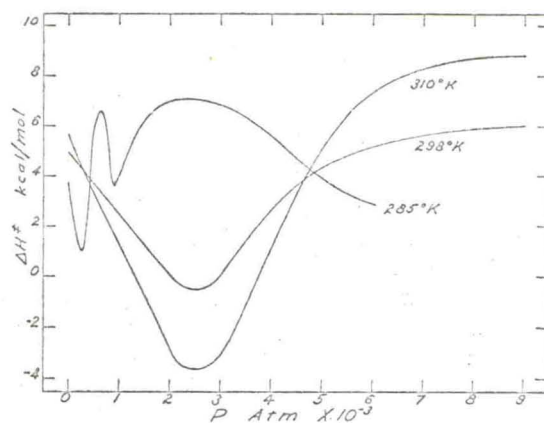


FIG. 3. Activation enthalpy as a function of pressure. System: THO-H₂O.

-1 N Na₂SO₄*

Observed D X 10 ⁴ cm ² /sec
0.28
0.33
0.29
0.39
0.56
0.91
0.55
0.90
1.01
0.86
0.76
1.07
1.60
0.78
1.03
0.80
4.86
1.24
1.14
1.34
1.88
2.24
2.27
1.46
1.26
1.81
1.54
1.25

verage deviation

.1 N K₂SO₄*

Observed D X 10 ⁴ cm ² /sec
0.33
0.67
0.71
0.50
0.40
0.90
0.86
0.83
0.82
0.66
1.40
0.98
1.04
1.30
1.44
0.90
0.84
1.17
1.59
0.82
0.87
3.92
2.48
0.87
0.75
1.46
2.06
2.37
1.44
1.04
0.58

verage deviation

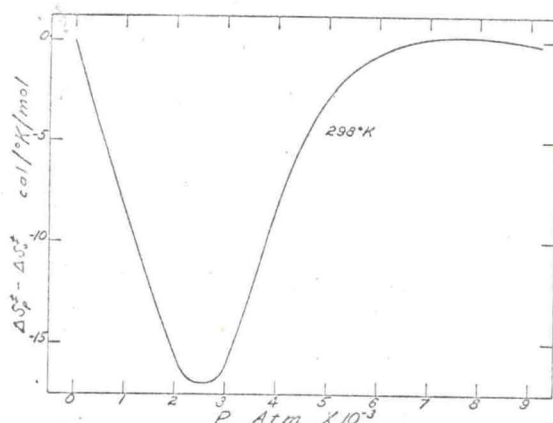


FIG. 4. Activation entropy as a function of pressure. System: THO-H₂O.

at 1 atmos. The minimum ΔS^\ddagger occurs in the same pressure region as does the zero activation volume. At this point the local expansion for activation becomes positive and the entropy of the activated state increases rapidly. The increase of ΔS^\ddagger continues (more gradually at higher pressure) until about 7000 atmos, where it levels to about the same value as at 1 atmos ($\Delta S_{P^\ddagger} - \Delta S_{0^\ddagger} \cong 0$). We saw above that the activation volume became virtually constant at this same pressure. The leveling of ΔS^\ddagger further substantiates the conclusion that a stabilized configuration has formed. Stabilized, that is, in the sense that the most probable configuration does not change greatly with pressure.

As a matter of general interest, $\Delta F_{P^\ddagger} - \Delta F_{0^\ddagger}$ was calculated at 25°. In Table VI below it is seen that the free energy of activation goes through a minimum at about 1500 atmos and then increases steadily. The total increase in 9000 atmos is 17 percent of ΔH_{0^\ddagger} ($\Delta H_{0^\ddagger} = 5000$ cal/mol).

From the isotherm of $\ln D$ in Fig. 1 it is seen that at 50° the diffusion coefficient decreases with the initial application of pressure as is normally expected. Thus, it appears that the tetrahedral structure does not control molecular motion to any prominent extent in the low pressure range at 50°. The activation volume increases from 45 percent of molal volume at 1 atmos to a maximum of 99 percent at 2000 atmos, while D continually decreases in this range. From this we infer that the decreasing free volume causes the local expansion necessary for activation to be felt over an increasingly larger portion of the liquid. Compressing beyond 2000 atmos the activation volume is seen to decrease rapidly and pass through zero to reach a minimum at 4200 atmos. At the same time, D drops rapidly beyond 1800 atmos, goes through a minimum at 3000, and rises slowly until a maximum is reached at 5800 atmos. These trends in the activation volume and diffusion coefficient lead to the conclusion that the free volume has been reduced to a point where, at 2000 atmos, the same situation is beginning to prevail as existed at 25° and 1 atmos. Namely, the tetrahedrally coordinated

structure controls the motion. D decreases more rapidly between 1800 and 2500 atmos because the average mobility of the molecules is decreasing as they become more and more tied up in the structure. Also, the activation volume decreases rapidly indicating that the activation process is beginning to involve collapse of the structure. Beyond 3000 atmos the structure begins to break down, the diffusion coefficient increases, and the major volume effect during activation becomes the localized collapsing of the structure so that ΔV^\ddagger becomes negative. $\Delta V^\ddagger/\bar{V}$ continues to decrease and goes through a minimum at 4200 atmos and then becomes zero again at 5800 where D is at a maximum. Above 5800 atmos the effect of whatever remains of the tetrahedral structure is no longer predominant, and the local expansion for diffusion becomes positive again. At 10 000 atmos $\Delta V^\ddagger/\bar{V}$ is 0.37 and appears to be leveling. It is anticipated that with further compression the activation volume would pass through a maximum and then settle to some constant lower value as the "stabilized" configuration is formed, as was the case at 25°.

It is to be noted in Fig. 3 that the enthalpy of activation is negative between 2300 and 2800 atmos at 298° and between 1400 and 3750 atmos at 310°. Even taking into consideration the tetrahedral structure and hydrogen bonding it is difficult to conceive of a situation wherein a molecule activated for diffusion would be at a lower energy level than it was in the initial state. It must be concluded then that the negative ΔH^\ddagger arises entirely as a result of the fact that at a given density the structure is radically different for the three widely separated isotherms we have studied.

At first glance one might feel that we have fixed the maximum and minimum in the low pressure range of the 0° isotherm with an insufficient amount of data (see Fig. 1). Although it is true that the position of these "critical" points may be shifted within the limits of experimental error, we are confident of their existence. The experimental runs were consistent within themselves, and also, other work on salt solutions (Figs. 7-9) has led us to expect such behavior in water and aqueous solutions. (See also the sulfuric acid data in Fig. 5.)

Since 0°C and 1 atmos is a triple point for water, it is to be expected that the liquid phase would contain large regions of the tetrahedrally coordinated structure in this pressure and temperature range. This accounts

TABLE VI. $\Delta F_{P^\ddagger} - \Delta F_{0^\ddagger}$ for self-diffusion in water at 25°C.

P (atmos)	$\Delta F_{P^\ddagger} - \Delta F_{0^\ddagger}$ (cal/mole)
500	-82
1000	-134
1500	-156
2000	-141
3000	-17
5000	416
7000	675
9000	843

for the fact that at 0° *D* rises from 1.45×10⁻⁵ at 1 atmos to a maximum of 2.35×10⁻⁵ in only 250 atmos (see Fig. 1). As rapidly as *D* rises to the maximum at 250 atmos, it falls again to a minimum of 1.06×10⁻⁵ at 600 atmos; ascends once more to a maximum of 1.85×10⁻⁵ at 900 beyond where it decreases gradually with pressure. The initial rise is explained by the same arguments used above concerning the breakdown of the structure and increase of mobility with pressure. The descent between 250 and 600 atmos must be caused by a secondary formation of the structure which ties up the molecules to decrease their mobility. Then once again this secondary structure suffers a breakdown with increasing pressure and *D* rises to its maximum at 900 atmos. The activation volume, plotted in Fig. 2, follows the same trends as would be expected on the basis of the arguments presented above for the 25° and 50° isotherms. At 1 atmos it is extremely negative, passes through zero at 250, becomes excessively large and positive, then descends to pass through zero at 600 atmos; between 600 and 900 atmos it goes extremely negative again and then ascends to some high positive value a little beyond 900 atmos. From this last positive maximum, $\Delta V^\ddagger/\bar{V}$ descends rapidly to 1.00 at 1000 and then more slowly to 0.36 at 2000 atmos. Beyond 2000 the descent is very gradual to 0.10 at 6000 atmos. It appears that with suitable compression, $\Delta V^\ddagger/\bar{V}$ would approach zero as an asymptote. From the gradual decline of *D* and of $\Delta V^\ddagger/\bar{V}$ beyond 2000 atmos it appears that the "stabilized" configuration is forming.

Bridgman³ gives data for the viscosity of water as a function of pressure at 0, 10.3, 30, and 75°C. He observed anomalous behavior at temperatures below 30°C in that the viscosity decreases with the initial application of pressure. The effect diminishes with increasing temperature. At 0° the viscosity at 1000 atmos is 92 percent of that at 1 atmos and then increases rapidly with pressure: at 10° a minimum of 95 percent of the value at 1 atmos is found at about 1200 atmos; no decrease is observed at 30 or 75° but the initial increase is very slow. These trends in the viscosity could be the result of breakdown of the tetrahedral water structure with increasing pressure and temperature. The effect is of a lesser extent and smaller magnitude than that we have observed in the case of diffusion. For all the

TABLE VII. The viscosity-diffusivity product for water.

Pressure atmos × 10 ⁻³	<i>D</i> η/η ₀ × 10 ⁻⁵	
	0°	25°
0	1.46	1.40
1	1.60	1.78
2	1.05	1.87
3	0.876	1.62
4	0.810	1.17
5	0.792	0.91
6	0.794	0.77
7		0.69
8		0.62
9		0.57

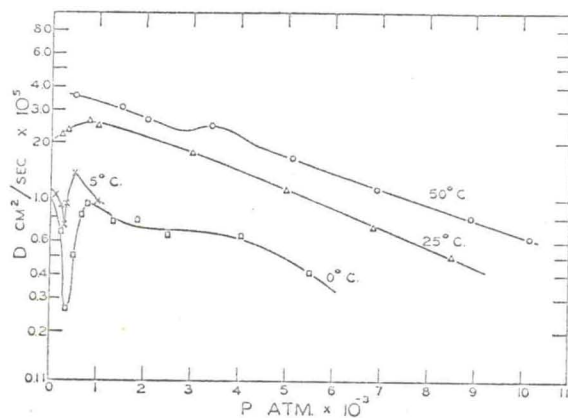


FIG. 5. Diffusion coefficients as a function of pressure. System: 0.1 N H₂SO₄-0.1 N H₂S²O₄.

systems we have studied it has been true that diffusion is more sensitive to pressure than is viscosity. The Stokes-Einstein equation predicts that the product of diffusion coefficient times the viscosity should be a constant. That this does not hold for water is seen in Table VII below where the product of the relative viscosity times the diffusion coefficient is shown for 25 and 0°C. The product may be approaching a constant value at 0° in the high pressure range.

0.1 NH₂S²O₄ IN 0.1 NH₂SO₄

Insofar as structure is concerned, the situation is probably much more complicated in sulfuric acid than in water. Along with having the tetrahedral water structure, the additional complication of solvation exists in the acid. The large size of the sulfate radical and its unbalanced valence forces probably cause further deviations from the water characteristics. It is impossible to give a unique interpretation to the diffusion data we have gathered. We shall not attempt to account for the effects of solvation or the sulfate radical but shall analyze the data giving consideration only to the characteristic tetrahedrally coordinated structure of water.

Isotherms of the diffusion coefficient are shown in a semilogarithmic plot against pressure in Fig. 5. Four temperatures were studied: 0, 5, 25, and 50°C. The ratio of the activation volume to the molal volume was calculated for the 0, 25, and 50° isotherms using compressibility data for water and is plotted in Fig. 6.

The isotherms in Fig. 5 show that *D* increases with the initial application of pressure at 25°C. Thus, it appears that the tetrahedral structure (modified by the acid) is a controlling factor for diffusion. Increasing pressure destroys the structure to increase the average sulfate mobility and *D* increases. The maximum value of *D* is found at about 900, and beyond this it decreases at a very steady rate with pressure. The activation volume (Fig. 6) is negative at one atmosphere and increases to pass through zero at about 900 atmos, where *D* was seen to be at a maximum. As in the case of water,

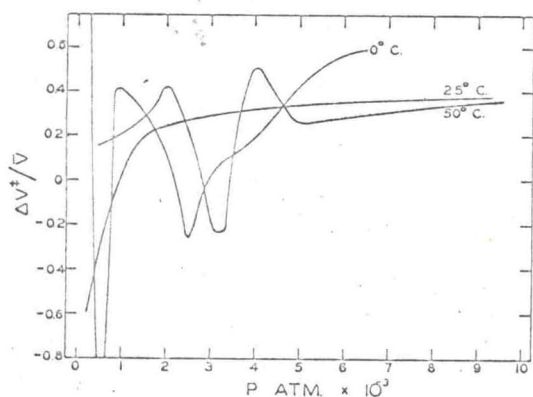


Fig. 6. Activation volumes as a function of pressure. System: 0.1 N H_2SO_4 -0.1 N $H_2S^{2}O_4$.

the negative ΔV^\ddagger indicates that diffusion takes place almost entirely by localized collapse of the tetrahedral structure. Compressing beyond 900 atmos the activation volume increases indicating a positive local expansion in the activation process which is felt through an increasingly larger portion of the liquid as the free volume is decreased. At 3000 atmos ΔV^\ddagger has become virtually constant and increases only slightly with pressure to about 37 percent of the molal volume at 9000 atmos. The steady decrease of D and the very gradual increase of $\Delta V^\ddagger/\bar{V}$ beyond 3000 atmos indicate that the average configuration in the liquid must be stable with pressure.

At 50°C the situation is qualitatively similar to water at 50°. At first the diffusion coefficient decreases with pressure indicating a normal activation process relatively unaffected by the tetrahedral structure. At 3500 atmospheres the diffusion coefficient increases with pressure, passes through a maximum, and decreases in a normal manner.

The 0 and 5° isotherms of D are quite erratic and much like water at 0°. The influence of whatever structure may exist at atmospheric pressure is rapidly increased with the initial compression. This is shown by the rapid decline of D from about 1.0×10^{-5} at 1 atm to about 0.27×10^{-5} at 335 atmos and 0°C. The sub-

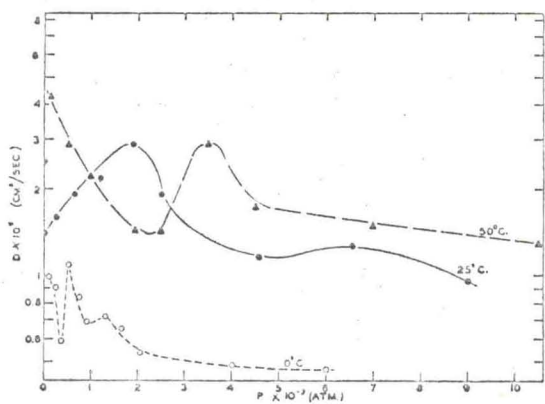


Fig. 7. Diffusion coefficients versus pressure 0.1 N Na_2SO_4 .

sequent ascent to a maximum of 0.95×10^{-5} at 840 atmos is equally rapid. Beyond 840 atmos D decreases and then settles to a plateau at 2000; at 3000 atmos it begins to decrease fairly rapidly again. In the range from 335 to 840 atmos the restricting configuration is apparently being broken down and D increases. At the 840 atmos maximum in D the tetrahedral structure no longer exists to a controlling extent, and we find the diffusion coefficient decreasing with pressure. The variation of the activation volume with pressure (Fig. 6) is consistent with our previous analysis.

It is seen in Fig. 5 that the 5° isotherm is similar to that for 0° as far as it was obtained (up to 1000 atmos).

The data for the three sulfate systems are shown in Tables III-V and Figs. 7-9. At first glance the results seem quite irregular, but the data were reproducible and very regular results were obtained for organic solutions on identical equipment. Extreme care was taken in nearly all cases to establish maximum and minimum points for the curves of diffusion coefficient versus

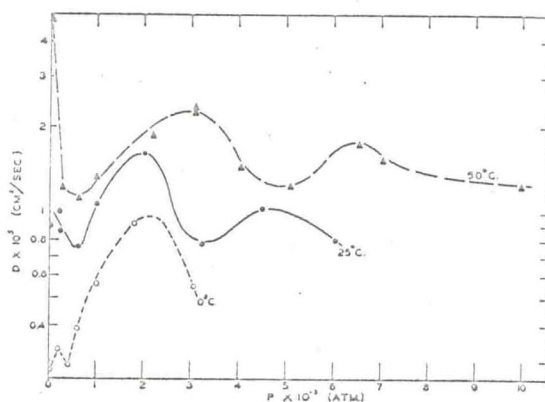


Fig. 8. Diffusion coefficients versus pressure in Na_2SO_4 .

pressure. This was accomplished either by making duplicate runs, or by making runs at small increments of pressure near what appeared to be a peak or dip in the curve. These check runs were found to reproduce the data within a maximum deviation of 10 percent.

Closer inspection of the original data do show very definite regularities, and these can be compared best by plotting the data of several isotherms together (Figs. 10-17) and are discussed in detail below. From these curves definite general conclusions can be obtained which are briefly stated at the end of the following paper.

50°C ISOTHERMS

A plot of diffusion coefficient versus pressure for the sulfate solutions and the water and sulfuric acid data² at 50°C is shown in Fig. 10. The similarities to the water curve are evident. It appears that in all but a small pressure range (2250-4250 atmospheres) the process of diffusion in water is faster and that the motion of molecules is governed by effects which may be regarded

as superimposed on the case of water. It is logically to be divided from atmospheric pressure to the first point to the first onward to the high

The minimum value for 1 N sodium sulfate and potassium sulfate and sulfate. This decrease in pressure is normal in this range involves of the surrounding evident from the low activation volume $\Delta V^\ddagger/\bar{V}_w$ (see Fig. 6) is greater than for sulfate solutions t

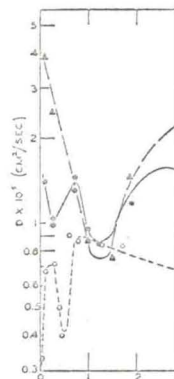


Fig. 9. Diffusion

largest for 1 N sodium sulfate and 0.1 N sodium sulfate. As the pressure increases and passes as the solution is essentially by local co

The activation function of the activation values for 0.1 N potassium sulfate for 0.1 N and 1 N sulfate. However, there is the of the activation exists which may corresponding atomic v

In the second range of activation volume largely due to the

In the pressure range for D , the value of while the activation zero for a short ra

² Hereafter this will

as superimposed on the factors that are influential in the case of water. Each of the three sulfate curves can logically be divided into three distinct sections, namely, from atmospheric pressure to the first minimum, from this point to the first maximum, and from this maximum onward to the highest pressure.

The minimum value for D occurs at 600 atmospheres for 1 N sodium sulfate, 1250 atmospheres for 0.1 N potassium sulfate and 2250 atmospheres for 0.1 N sodium sulfate. This decrease in D with initial application of pressure is normally expected, and molecular motion in this range involves, to a large extent, the pushing back of the surrounding medium as in normal liquids. It is evident from the slopes of the diffusion coefficient curves in this low pressure region that the ratio of activation volume to the molar volume of water, $\Delta V^\ddagger/\bar{V}_w$, (see Fig. 11) for the aqueous sulfate solutions is greater than for water and is positive. Within the sulfate solutions the initial activation volume ratio is

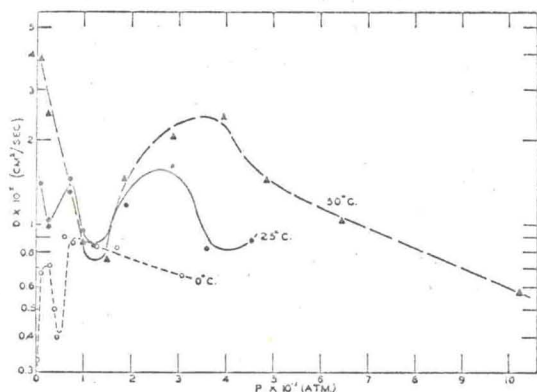


FIG. 9. Diffusion coefficients versus pressure 0.1 K₂SO₄.

largest for 1 N sodium sulfate followed by 0.1 N potassium sulfate and 0.1 N sodium sulfate, respectively.

As the pressure increases, the activation volume decreases and passes through a minimum, indicating that as the solution is compressed motion takes place preferentially by local collapse of the tetrahedral structure.

The activation volume ratio does not seem to be a function of the atomic volume of the cation, because the values for 0.1 N potassium sulfate lie between the values for 0.1 N and 1 N sodium sulfate, respectively. However, there is the possibility that a regular dependency of the activation volume ratio on the solvated volume exists which may be radically different from the corresponding atomic volumes of the cations.

In the second region, where D is increasing and the activation volume is negative, motion is apparently largely due to the local collapse of the structure.

In the pressure range beyond the last maximum value for D , the value of D decreases at a relatively slow rate while the activation volume ratio increases beyond zero for a short range, passes through a maximum, and

⁶ Hereafter this will be referred to as the activation volume ratio.

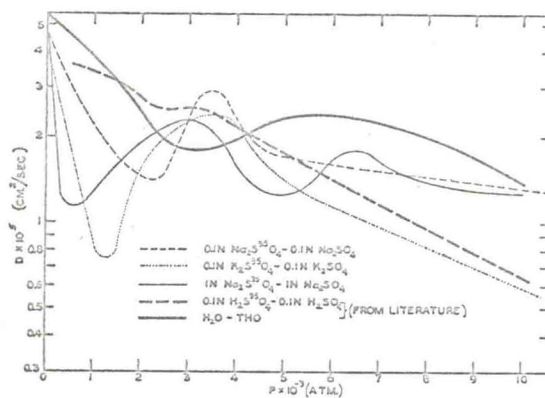


FIG. 10. Diffusion coefficients versus pressure sulfate solutions at 50°C.

then decreases at a decreasing rate which asymptotically approaches 0.08 for 1 N sodium sulfate, 0.10 for 0.1 N sodium sulfate, and 0.20 for 0.1 N potassium sulfate. These trends indicate that either the tetrahedral structure is completely destroyed, or the effect of the increased compactness of the medium is greater than the effect of whatever structure remains or any new structure which may have formed. Whichever the case may be, it is apparent that as the pressure is increased in this region a stabilized arrangement is forming and diffusion of the molecules is taking place more and more through the interstices which are not rapidly decreasing in size with pressure.

The irregularity in the 1 N Na₂SO₄ solution in the high pressure range may be due to ionic interaction at the higher concentration or to an additional desolvation effect not present at the lower concentrations.

25°C ISOTHERMS

The plots for the diffusion coefficient, activation volume ratio, activation enthalpy, and activation entropy⁶ for the sulfate solutions and water and sulfuric acid are shown in Figs. 12, 13, 14, and 15, respectively. The activation volume ratio is obtained for each iso-

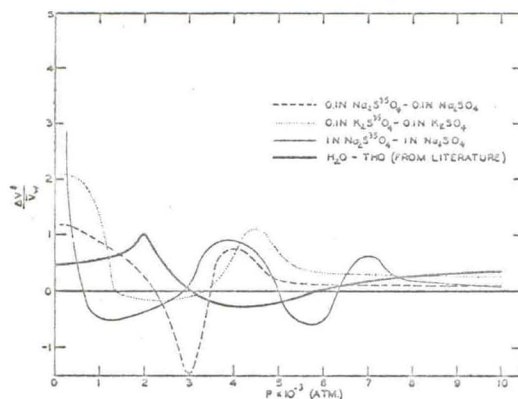
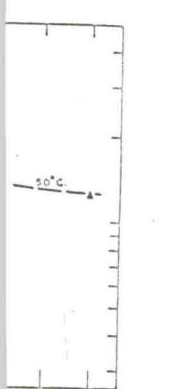


FIG. 11. Activation volume ratios for sulfate solutions at 50°C.

⁶ This term will be used in place of $\Delta S_p^\ddagger - \Delta S_0^\ddagger$.

$\times 10^{-5}$ at 840
as D decreases
3000 atmos it
the range from
uration is ap-
pears. At the
structure no
d we find the
pressure. The
pressure (Fig. 6)

n is similar to
10000 atmos).
are shown in
nce the results
e reproducible
r organic solu-
are was taken
and minimum
efficient versus



n Na₂SO₄.

by making
all increments
peak or dip in
to reproduce
0 percent.
to show very
pared best by
gether (Figs.
From these
be obtained
the following

ssure for the
ic acid data³
to the water
but a small
the process
e motion of
be regarded

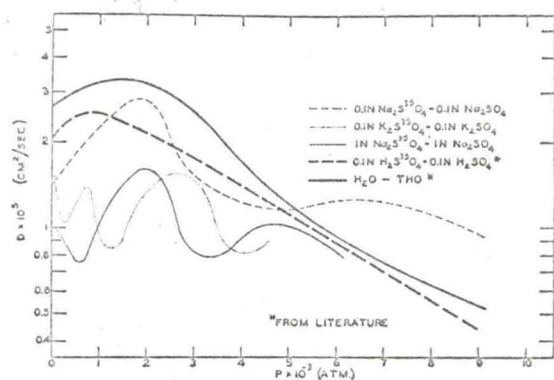


Fig. 12. Diffusion coefficients *versus* pressure sulfate solutions at 25°C.

therm independently, while the activation enthalpy and entropy depend on the displacement between two or more isotherms. Inasmuch as the structure of the solution varies widely with temperature, the activation enthalpy and entropy calculated probably do not apply to any one isotherm.

The similarity between water, 0.1 *N* H₂SO₄ and 0.1 *N* Na₂SO₄ are evident from Figs. 12 and 13, but the 1*N* Na₂SO₄ and 0.1 *N* K₂SO₄ have additional maxima and minima which are not easily explainable but which are definitely present.

In the low pressure region the increase in *D* and the negative activation volume indicate that the tetrahedral structure collapses locally during molecular motion. At pressures beyond the point where the collapse of structure dominates the motion of molecules, the water and sulfuric acid display a high degree of regularity associated with normal liquids. However, in this region the sulfate curves show irregularities, i.e., additional maxima and minima, which probably could be explained on the basis of the pressure dependency of desolvation and ionic interaction.

In the high pressure region Figs. 11 and 13 show that the activation volume ratios for all the solutions asymptotically approach approximately the same relatively low value, indicating a similarly stable structure for all solutions at very high pressure at both 25° and 50°C.

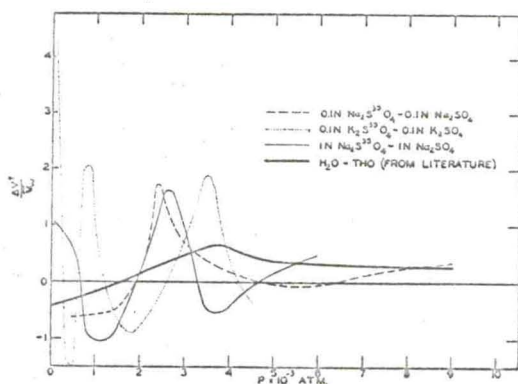


Fig. 13. Activation volume ratios for sulfate solutions at 25°C.

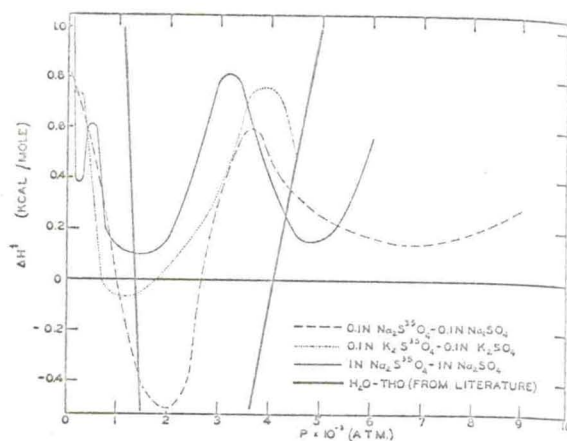


Fig. 14. Activation enthalpies for sulfate solutions at 37.5°C.

0°C ISOTHERMS

Figures 16 and 17 are plots of diffusion coefficients and activation volume ratios, respectively, *versus* pressure for the sulfate solutions and water and sulfuric acid.

There is a definite similarity between these sulfate curves and the water curve, and the similarity is even clearer between the sulfuric acid and 0.1 *N* sodium sulfate and among the water, 0.1 *N* potassium sulfate, and 1 *N* sodium sulfate.

In the very low pressure range, it appears that molecular motion is influenced by the more rigid structure that exists at 0°C. With the exception of the increase of *D* with pressure for the 1 *N* sodium sulfate and 0.1 *N* potassium sulfate in the initial pressure range, the curves all show the value of *D* decreasing to a minimum, rising to a maximum and dropping off in the high pressure range.

Molecular motion in the region where *D* initially decreases is controlled by the decrease in free volume, and the rigid structure at 0°C remains so and does not undergo any pronounced rearrangement with the initial application of pressure. Beyond the pressure where *D* is maximum, there is a general decrease in the value of *D* and an asymptotic leveling of the activation volume

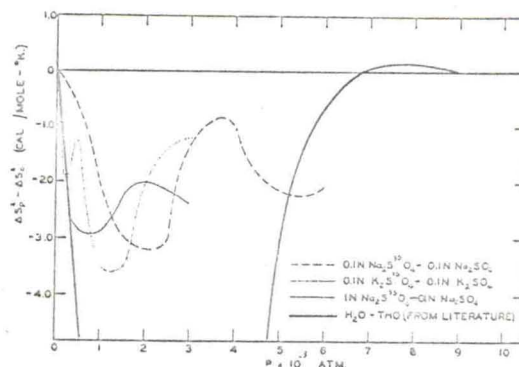


Fig. 15. Activation entropies for sulfate solutions at 25°C.

Fig. 16.

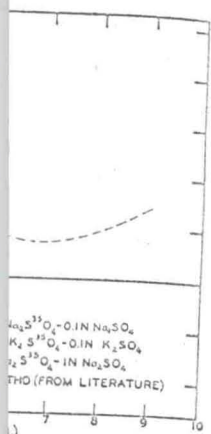
ratio to r
the activ
variations
1000 atm
plotted. I
the forma
and sulfa

The co
solutions
conducta

* W. A.

THE J

D
aque
75°C
TIN
a 0.0
In
The
Oak
End
The
Cor

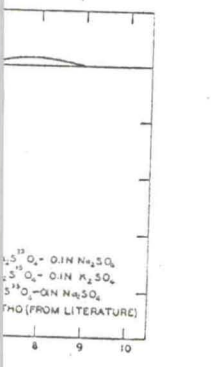


solutions at 37.5°C.

diffusion coefficients respectively, versus pressure for water and sulfuric acid solutions. Between these sulfate solutions, the similarity is even greater for 0.1 N sodium and potassium sulfate,

it appears that the more rigid structure of sodium sulfate and in the pressure range, increasing to a minimum off in the high

where *D* initially increases in free volume, as so and does not depart with the initial pressure where *D* is in the value of *D* activation volume



solutions at 25°C.

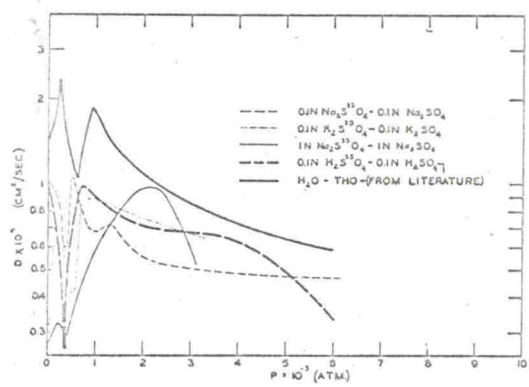


Fig. 16. Diffusion coefficients for sulfate solutions at 0°C.

ratio to relatively small values (Fig. 17). Inasmuch as the activation volume ratios are extreme and their variations are compressed in the pressure range below 1000 atmospheres, only the high pressure values are plotted. It is this portion of the curves that indicate the formation of similarly stable structures for water and sulfate solutions.

The conductivity data of Zisman⁷ on 0.01 *N* salt solutions (including Na₂SO₄) shows a maximum in the conductance at about 1000 atmospheres, followed by a

⁷ W. A. Zisman, Phys. Rev. 39, 151 (1932).

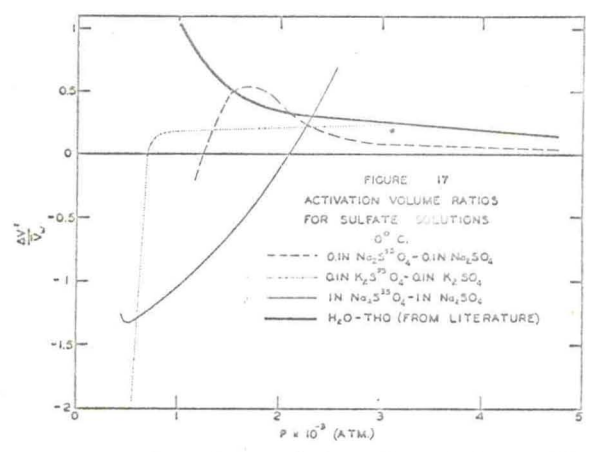


Fig. 17. Activation volume ratios for sulfate solutions at 0°C.

linear decrease. The lack of detailed structure may be due to the decreased concentration or to the lack of sensitivity of conductance.

R. B. Cuddeback would like to acknowledge assistance from the Shell Fellowship Committee and from the U. S. Atomic Energy Commission.

R. C. Koeller would like to acknowledge assistance from the Pan American Refining Corporation and the U. S. Atomic Energy Commission.

The Effect of Pressure on Diffusion in Aqueous and Alcoholic Salt Solutions*

R. B. CUDDEBACK AND H. G. DRICKAMER

Department of Chemistry, University of Illinois, Urbana, Illinois

(Received August 26, 1952)

Diffusion coefficients have been measured as a function of pressure to 10 000 atmos for the following aqueous solutions:

- 0.1 *N* Hg(NO₃)₂ at 0°, 25°, 50°, 75°C,
- 0.1 *N* CaCl₂ at 25°, 50°C,
- 0.1 *N* Ca(NO₃)₂ at 25°C,
- 0.1 *N* TiNO₃ at 25°C,

and for 0.01 *M* HgCl₂ in *n*-butanol at 25° and 50°C. The results are interpreted in terms of the activation volume, and compared with previous data on water and sulfate solutions.

DIFFUSION coefficients have been measured as a function of pressure to 10 000 atmos in 0.1 *N* aqueous solutions of Hg(NO₃)₂ at 0°, 25°, 50°, and 75°C; CaCl₂ at 25° and 50°C; Ca(NO₃)₂ at 25°C; and TiNO₃ at 25°C. Measurements have also been made in a 0.01 *M* HgCl₂ in *n*-butanol solution.

In every case a radioactive tracer technique was used. The tracers (Hg²⁰³, Ca⁴⁵, Ti²⁰⁴) were obtained from Oak Ridge National Laboratory of the U. S. Atomic Energy Commission. The salts were of cp quality. The *n*-butanol was purchased from Eastman Kodak.

* This work was supported in part by the U. S. Atomic Energy Commission.

The experimental procedures, method of calculation of the diffusion coefficient, and the general theory have been previously discussed.^{1,2,3}

The results are presented in Tables I-V and Figs. 1-5. These will be discussed under four headings; mercuric nitrate, comparison of nitrate isotherms, calcium chloride isotherms, and mercuric chloride-butanol isotherms.

¹ R. C. Koeller and H. G. Drickamer, J. Chem. Phys. 21, 267 (1953).

² R. C. Koeller and H. G. Drickamer, J. Chem. Phys. 21, 575 (1953).

³ Cuddeback, Koeller, and Drickamer, J. Chem. Phys. 21, 589 (1953)